Supplementary Information

An intrinsic self-healable supramolecular dynamic covalent elastomer for sustainable high-performance tactile sensing

Ding Yang, Jiahui Zhao, Fang-Yu Liu, Meng Chen and Da-Hui Qu**

Key Laboratory for Advanced Materials and Joint International Research Laboratory of Precision Chemistry and Molecular Engineering, Feringa Nobel Prize Scientist Joint Research Center, Frontiers Science Center for Materiobiology and Dynamic Chemistry, Institute of Fine Chemicals, School of Chemistry and Molecular Engineering, East China University of Science and Technology, 130 Meilong Road, Shanghai, 200237 (China).

*Corresponding author: ac0105@ecust.edu.cn, dahui_qu@ecust.edu.cn

Table of Contents

Experimental

Monomer fabrication

All chemicals were obtained from Sigma-Aldrich and MACKLIN, China, and used as received without further purification. TA (1.1 eq, 1.0 g, 4.85 mmol) and SPG (1.0 eq, 3.0 g, 4.4 mmol) were dissolved in DCM (100 mL). DMAP (0.11 eq, 0.059 g, 0.49 mmol) and EDCI (1.1 eq, 0.95 g, 4.85 mmol) were added to the DCM solution. The mixture was stirred at room temperature for 12 h. The product was purified by column chromatography (silica gel, PE/EA = 1) to afford compound SPG (yield = 86%) as a yellow solid.

Polymer fabrication

High power LED lamp source (Beijing Perfectlight: PLS- LED100C) (365 nm) with 50 W power was utilised to obtain photo-polymerised polymers.

The polymers were fabricated as: 0.48 g of SPG and 2 g of TA powder were combined and heated at 120°C. The liquid mixture was exposed to ultraviolet light (365 nm) for 12 hours for a yellow transparent solid. The preparation process for the other copolymers used in subsequent tests followed the same method as described above.

Structure characterisations

Chemicals were weighed on analytical balances (METTLER- TOLEDO, ME204T/02). Nuclear magnetic resonance (NMR) spectrum was tested by Brüker AV-400 (^{1}H NMR) and AV-600 (^{13}C NMR) spectrometer using tetramethylsilane to be the internal standard. The electronic spray ionisation (ESI) mass spectra were tested on an LCT Premier XE mass spectrometer. The Raman spectra were recorded using a Laser Micro-Raman Spectrometer (Renishaw, I0.2/cm/invia reflex) equipped with a high-performance grade Leica DMLM microscope and a 785 nm excitation wavelength. X-ray diffraction (XRD) patterns were obtained on a rotating anode X-ray powder diffractometer (18KW/D/max2550VB/PC) equipped with a copper target 18KW (450 mA), a fully automated curved (plate) crystal graphite monochoromator and a programmed variable slit system. Fourier transform infrared spectrometer (FT-IR) (Thermo Nicolet Corporation; 7800- 350/cm 0.01/cm/6700) was used to analyse the copolymer samples.

Thermal properties tests

The thermal stability was measured by thermogravimetric analysis (Mettler Toledo TGA/SDTA851, heating rate = 5°C min^{-1}). The thermal properties were measured by differential scanning calorimetry (TA instruments; modulated DSC2910, 1090B, ramp rate = 5°C min^{-1}).

Mechanical properties tests

The mechanical properties of the polymer films were measured by an HY-0580 tension machine (HENGYI). The rheological experiments were performed by rotational rheometer (TA Instruments- Waters LLC; DHR-2). All stress-strain curves were obtained from a HY-0580 tension machine (HENGYI Company). The rectangular test samples (30 × 5 × 0.5 mm) were fixed on the jigs of the tension machine, with the initial length (10 mm) considered as the gap between the two edges of the jigs. Unless otherwise noted, the tensile stress was measured at a constant speed of 20 mm min^{-1}.

Self-healing experiment

The self-healing experiment was done as follows: the rectangle-shaped tested sample (length, 30 mm; width, 10 mm) was cut off into two identical pieces by a knife from the middle. Then the interfaces of the two pieces were contacted immediately followed by slight extrusion. The reassembled sample was placed for different hours before a test at room temperature. The testing procedure was the same as above. The polarised optical microscopy images were obtained on typical optical microscopy equipped with two polarisers. Different humidity test was conducted as follows: the 0% RH condition was to put freshly prepared polymer samples in a desiccator for three consecutive days prior to tensile test, representing winter-like conditions; the 50% RH condition was established by exposing the samples to ambient laboratory air for three days, corresponding to typical spring or fall conditions; the 70% RH condition, simulating summer conditions, was realized using a custom-designed humidity-controlled chamber.

Recycled tests

The virgin polymer chips (1 g) were chopped, added into chloroform with the presence of Triflic acid TfOH (0.03 g). The mixture was heated to 70°C for 8 hours until a clear transparent yellow even solution was obtained, washed with water (10 ml × 5), saturated sodium chloride (10 ml

× 2), then concentrated. A bright yellow recycled monomeric solid was obtained, then subjected to polymer fabrication as described above.

Sensor tests

The relative capacitance changes in the elastomers with pressure were recorded by digital source meter TH2830 LCR Test System 2.2.12D@170522. The relative capacitance change was calculated according to the following equations: $\Delta C/C_0 = (C-C_0)/C_0$, $S = (\Delta C/C_0)/P$, where C is the real-time capacitance of the stretched elastomer at a certain state and C_0 is the original capacitance. The S was calculated to assess the sensing sensitivity of the elastomer, and P is the pressure imposed on the elastomer. All experiments were performed in accordance with the Guidelines of the Measures for Ethical Review of Life Science and Medical Research Involving Human Beings Article 32, and approved by the ethics committee at The East China University of Science and Technology. Informed consents were obtained from human participants of this study.

Section I. Monomer spectrum assignment

Monomer **SPG**

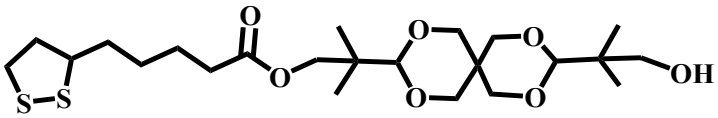

Figure S1. Graphic presentation of monomeric precursor compound SPG.
^{1}H NMR (400 MHz, Chloroform-*d*, 298 K) δ (ppm): 4.50 (ddd, *J* = 11.5, 6.3, 2.6 Hz, 1H), 4.24 (d, *J* = 6.2 Hz, 1H), 3.91 (s, 1H), 3.63 – 3.05 (m, 6H), 2.50 – 2.26 (m, 1H), 1.97 – 1.38 (m, 3H), 1.25 (d, *J* = 12.5 Hz, 0H), 0.98 – 0.86 (m, 6H).
^{13}C NMR (151 MHz, Chloroform-*d*, 298 K) δ (ppm): 108.10, 105.02, 78.63 – 75.87 (m), 71.23 – 68.73 (m), 56.40, 40.65 – 37.98 (m), 34.15, 32.65 (d, *J* = 11.1 Hz), 28.82, 24.77, 20.58 – 18.78 (m).
HR-MS (ESI) (*m/z*): $[M + H]^+$ calcd. For $C_{23}H_{41}NaO_7S_2$, 493.2294, found 493.2288, (680.2545 or m/z 680.9890).

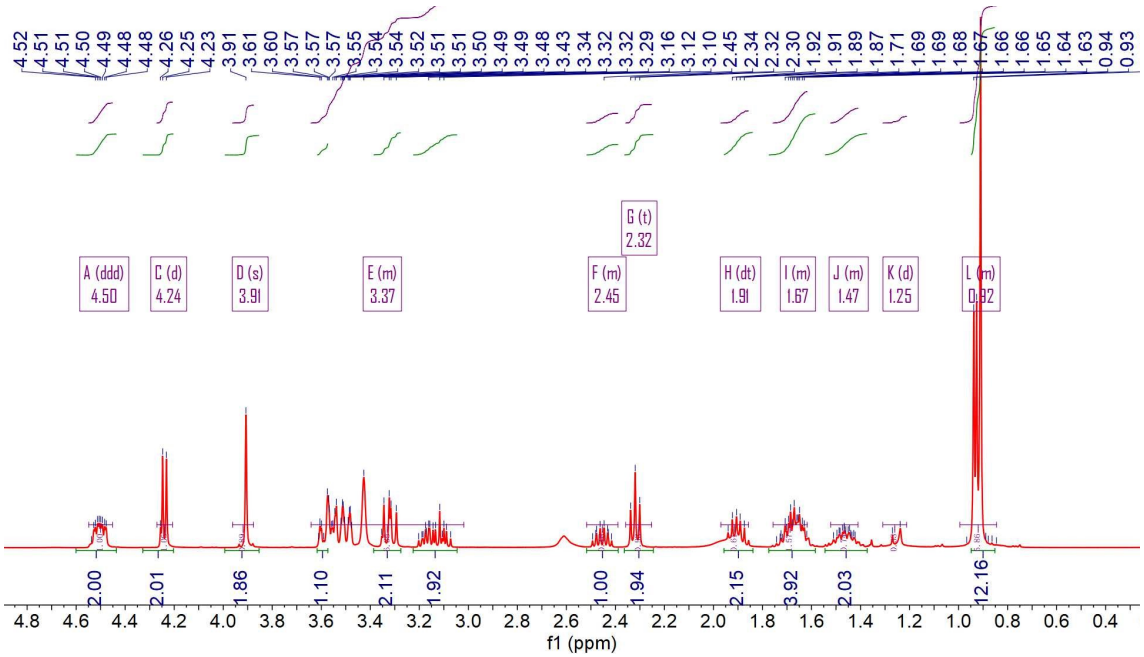

Figure S2. ^{1}H NMR spectrum of **SPG** monomer. (400 MHz, $CDCl_3$, 298 K)

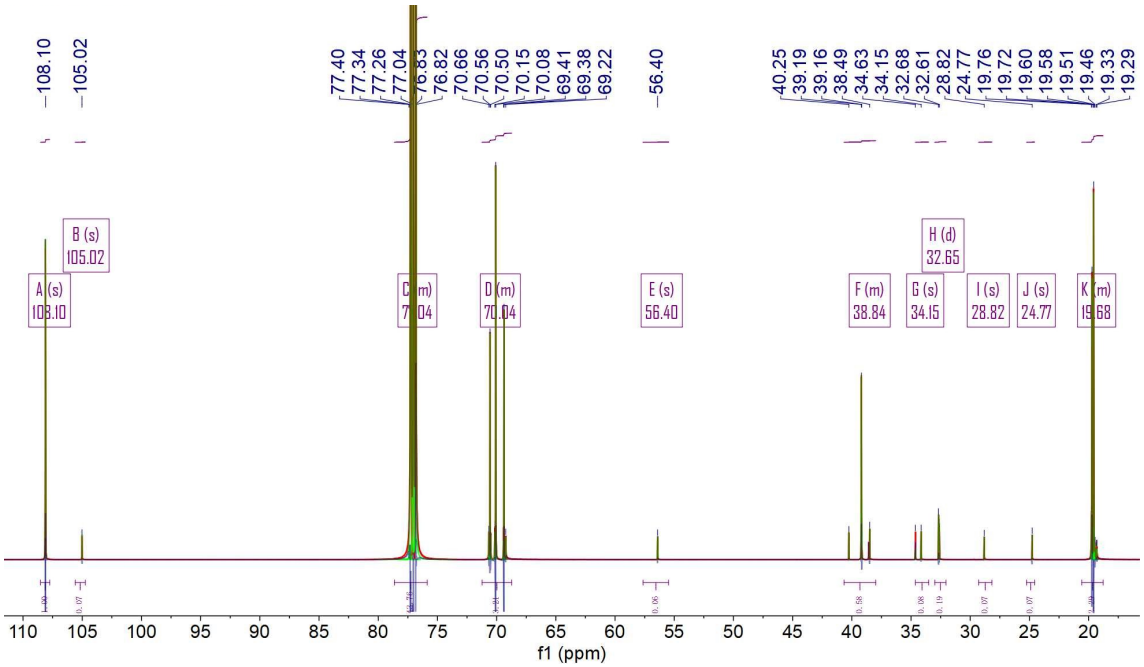

Figure S3. ^{13}C NMR spectrum of **SPG** monomer. (600 MHz, $CDCl_3$, 298 K)

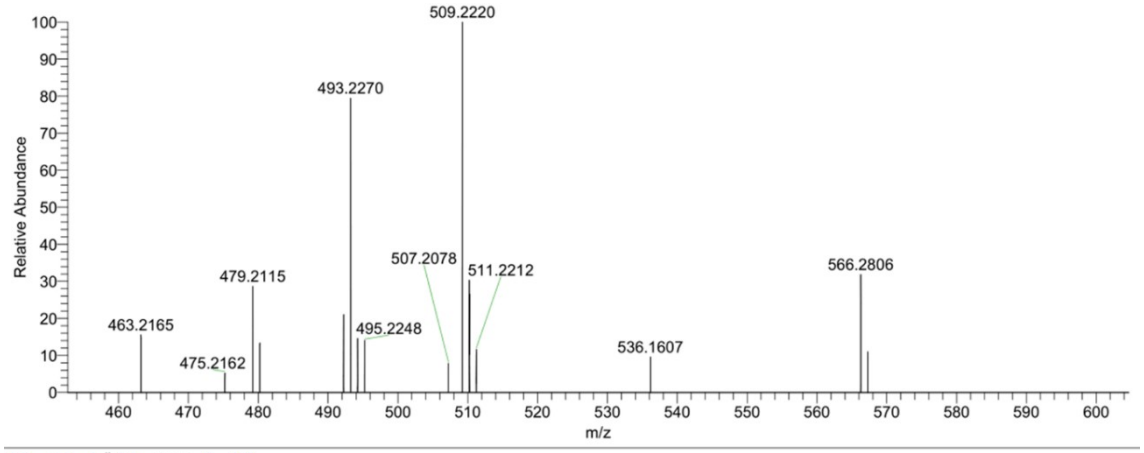

QD-YD-1#81 RT: 0.19
T: FTMS + p NSI Full ms [100.0000-1500.0000]
m/z= 493.14-493.35

m/z	Intensity	Relative	Theo. Mass	Delta (ppm)	Composition
493.2270	38120.9	100.00	493.2288	-1.80	$C_{23}H_{41}O_7S_2$

Figure S4. Mass spectrum of **SPG** monomer.

Section II. Supporting Figures

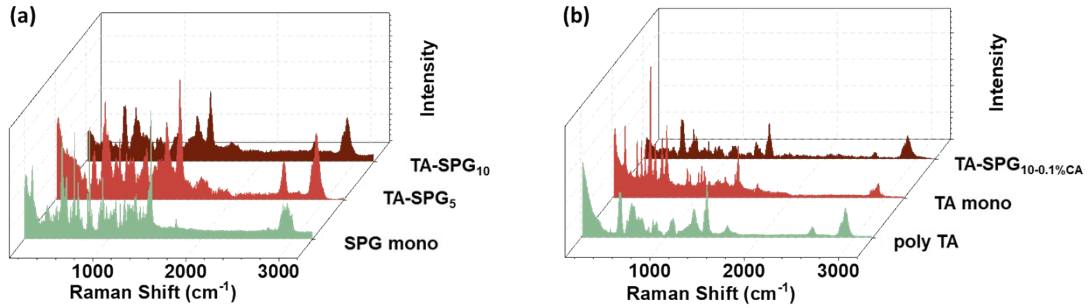

Figure S5. Raman spectra of **TA-SPG** polymers.
(a) **SPG mono, TA-SPG$_5$,** and **TA-SPG$_{10}$.** (b) **poly TA, TA mono,** and **TA-SPG$_{10\text{-}0.1\%CA}$.**

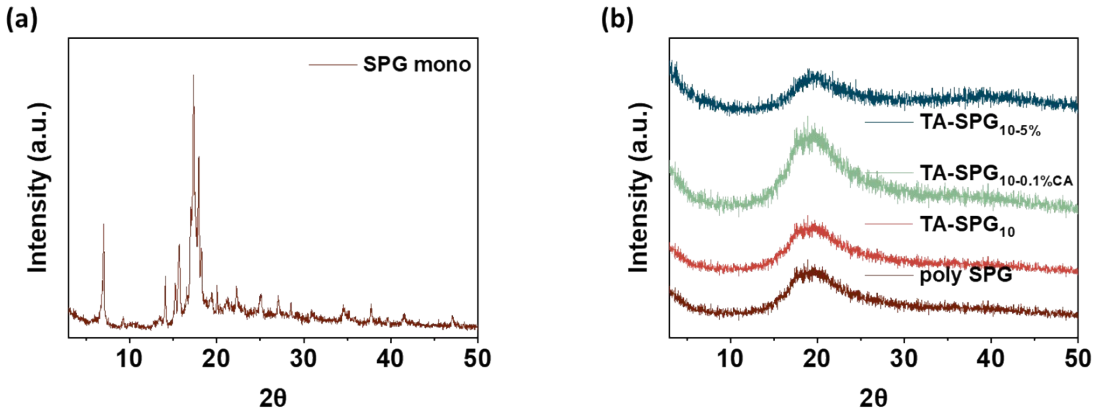

Figure S6. X-ray diffraction (XRD) of **TA-SPG** polymers.
(a) **SPG mono**. (b) **TA-SPG$_{10\text{-}5\%}$**, **TA-SPG$_{10\text{-}0.1\%CA}$**, **TA-SPG$_{10}$**, and poly **SPG**.

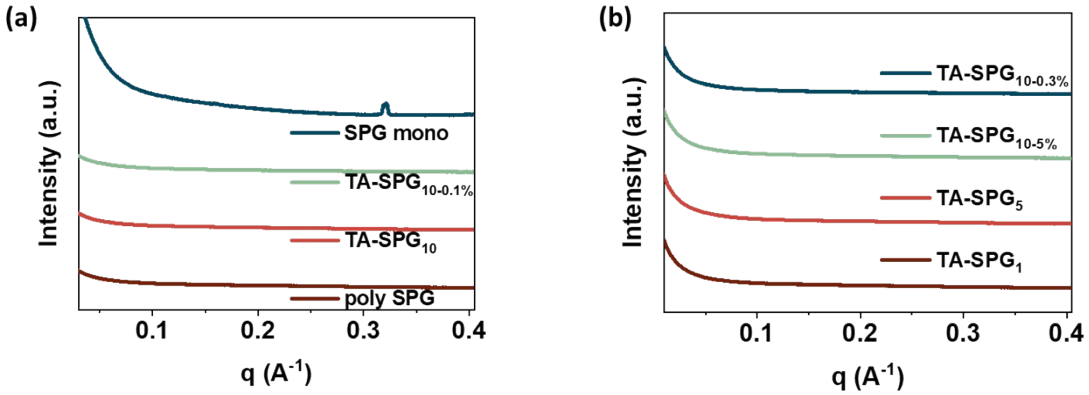

Figure S7. Synchrotron-radiation small-angle X-ray scattering (SAXS) of **TA-SPG** polymers.
(a) **poly SPG**, **TA-SPG$_{10}$**, **TA-SPG$_{10\text{-}0.1\%}$**, **SPG mono**. (b) **TA-SPG$_1$**, **TA-SPG$_5$**, **TA-SPG$_{10\text{-}5\%}$**, **TA-SPG$_{10\text{-}0.3\%}$**. Synchrotron-radiation small-angle X-ray scattering (SAXS) measurements confirmed the amorphous network without notable microphase separation.

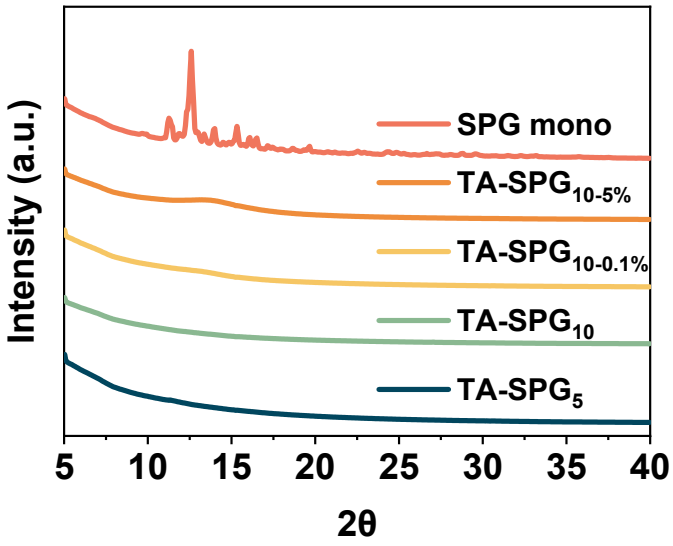

Figure S8. Wide-angle X-ray scattering (WAXS) of **TA-SPG** polymers.
TA-SG$_5$, **TA-SG$_{10}$**, **TA-SG$_{10\text{-}0.1\%}$**, **TA-SG$_{10\text{-}5\%}$**, **SPG mono.** Wide-angle X-ray scattering (WAXS) measurements confirmed the amorphous network without notable microphase separation.

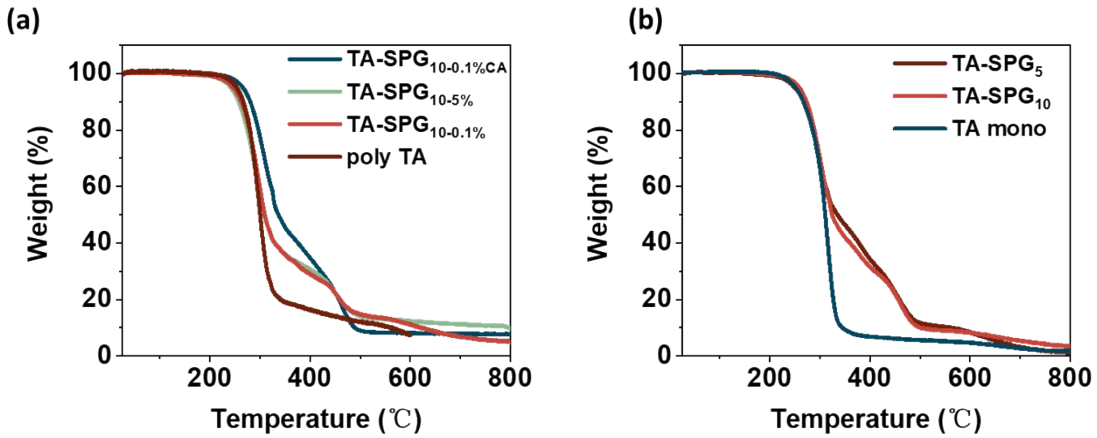

Figure S9. Thermogravimetry analysis (TGA) of **TA-SPG** polymers.
(a) **TA-SPG$_{10\text{-}0.1\%CA}$**, **TA-SPG$_{10\text{-}5\%}$**, **TA-SPG$_{10\text{-}0.1\%}$**, **poly TA**. (b) **TA-SPG$_5$**, **TA-SPG$_{10}$**, **TA mono.** Different scales polymers of **TA** and **SG** show an obvious enhancement at decomposition temperature from TGA data. There is little difference among the decomposition curves of different amounts of additives [CA: Fe].

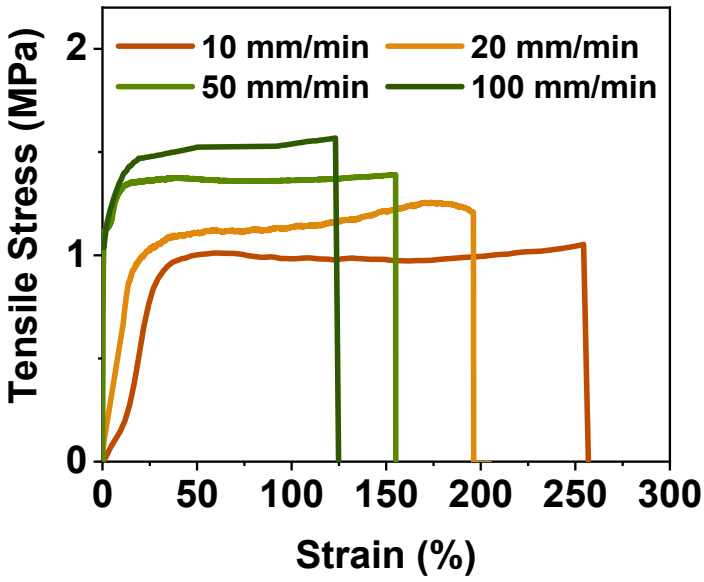

Figure S10. The tensile stress-strain curves with different rates of **TA-SPG$_{10\text{-}0.1\%}$.**

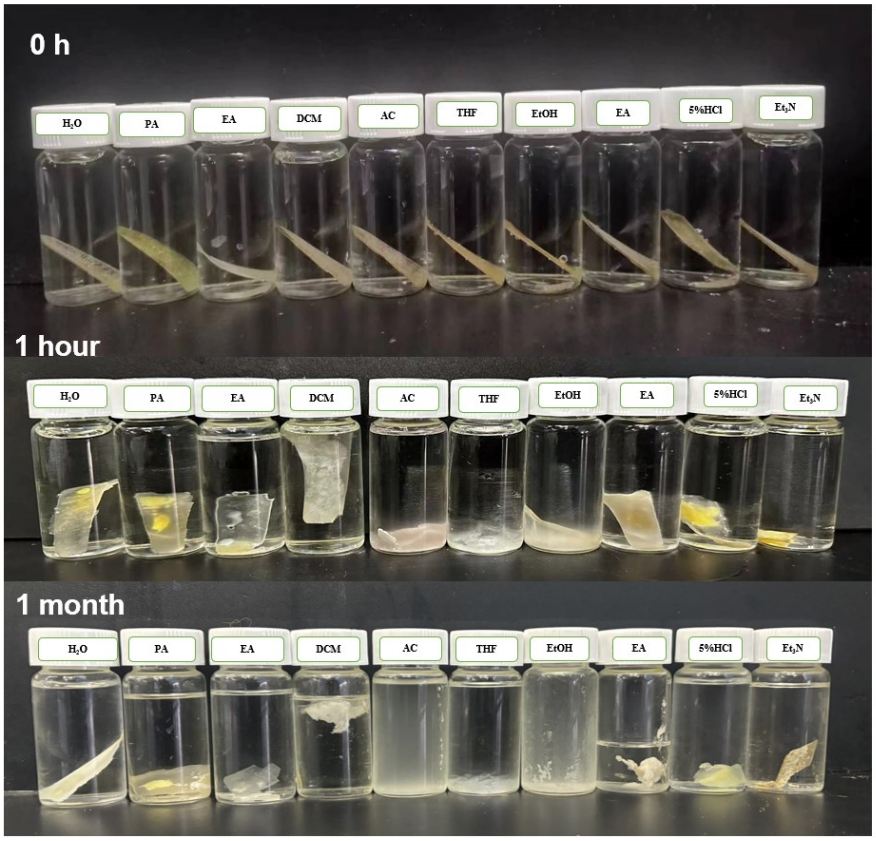

Figure S11. Swelling experiments of **TA-SPG$_{10\text{-}0.1\%}$** polymer. photos of **TA-SPG$_{10\text{-}0.1\%}$** polymers in different solvents.

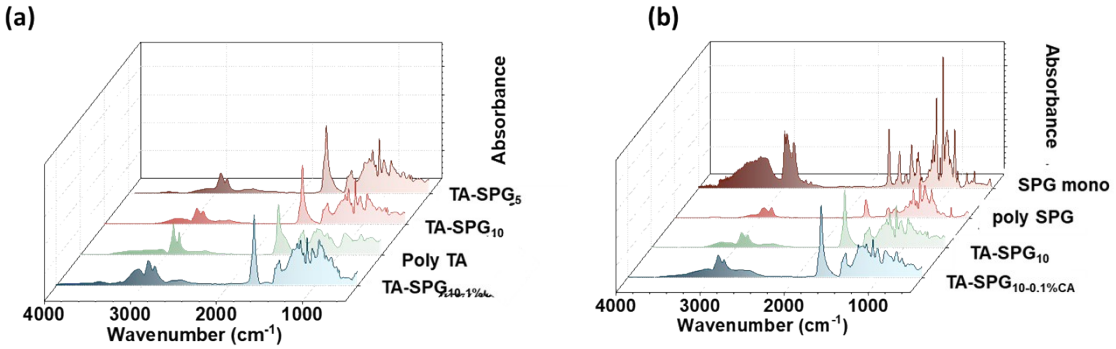

Figure S12. The attenuated total reflection Fourier-transform infrared (ATR-FTIR) spectra of polymers.

(a)The attenuated total reflection Fourier-transform infrared (ATR-FTIR) spectra of **TA-SPG$_1$**, **TA-SPG$_5$**, **TA-SPG$_{10\text{-}5\%}$**, **TA-SPG$_{10\text{-}0.1\%CA}$**. (b)The attenuated total reflection Fourier-transform infrared (ATR-FTIR) spectra of **TA-SPG$_{10\text{-}0.1\%CA}$**, **TA-SPG$_{10}$**, **poly SPG, SPG mono**.

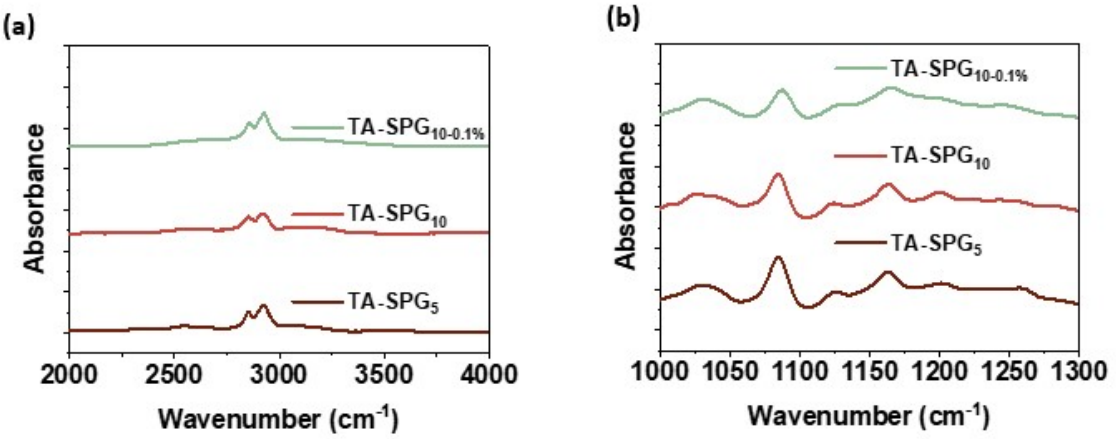

Figure S13. The attenuated total reflection Fourier-transform infrared (ATR-FTIR) spectra of polymers.

(a-b) (a)The attenuated total reflection Fourier-transform infrared (ATR-FTIR) spectra of **TA-SPG$_5$**, **TA-SPG$_{10}$**, **TA-SPG$_{10\text{-}0.1\%}$**, (a) from 2000 to 4000 cm^{-1} and (b) from 1000 to 1300 cm^{-1}.

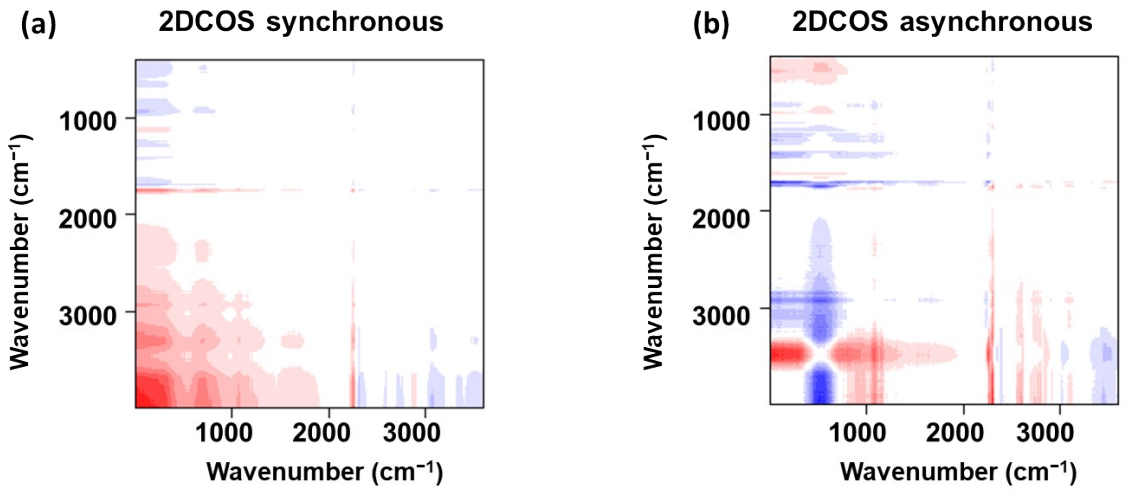

Figure S14. Two-Dimensional Correlation Spectroscopy (2D-COS).
(a) Two-Dimensional Correlation Spectroscopy (2D-COS) synchronous and (b) Two-Dimensional Correlation Spectroscopy (2D-COS)asynchronous spectra. The red color represents positive spectral intensities, while the blue color represents negative ones.

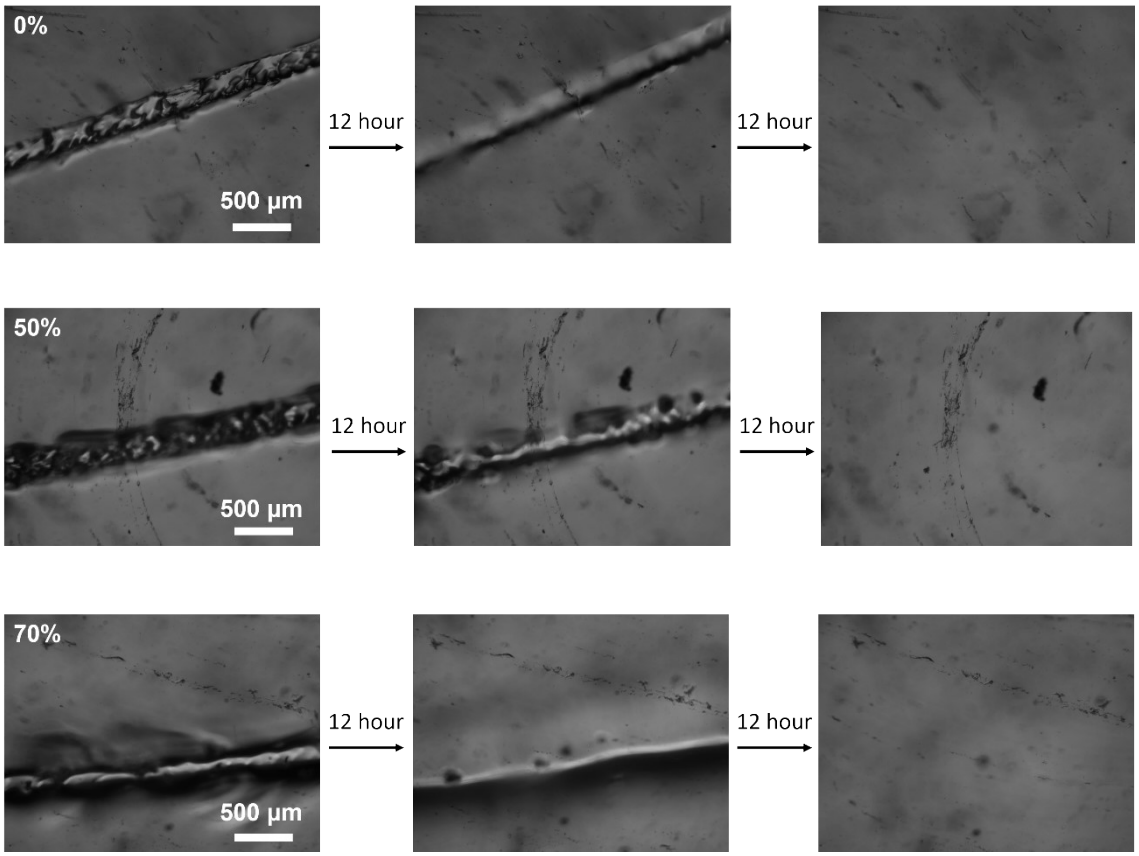

Figure S15. The self-healing progress of **TA-SPG$_{10\text{-}0.1\%}$** under different ambient humidity conditions by optical microscopy.

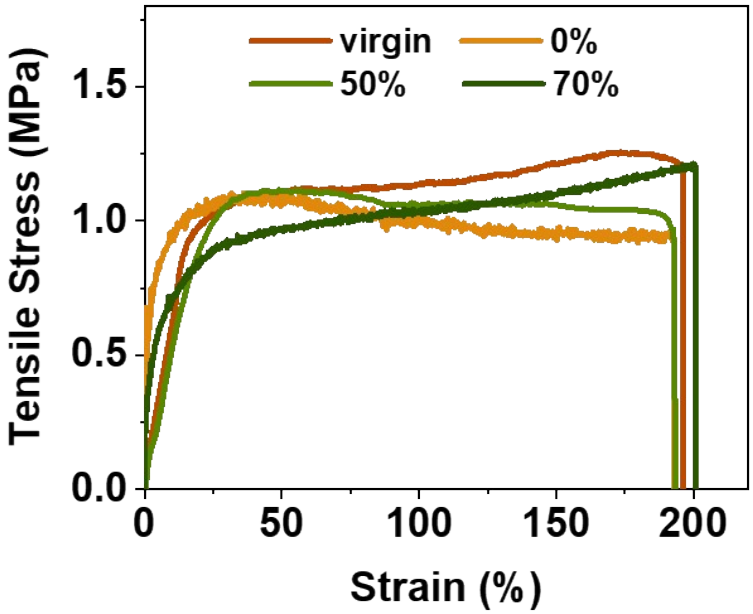

Figure S16. The tensile testing of **TA-SPG$_{10\text{-}0.1\%}$** after self-healing under different ambient humidity conditions.

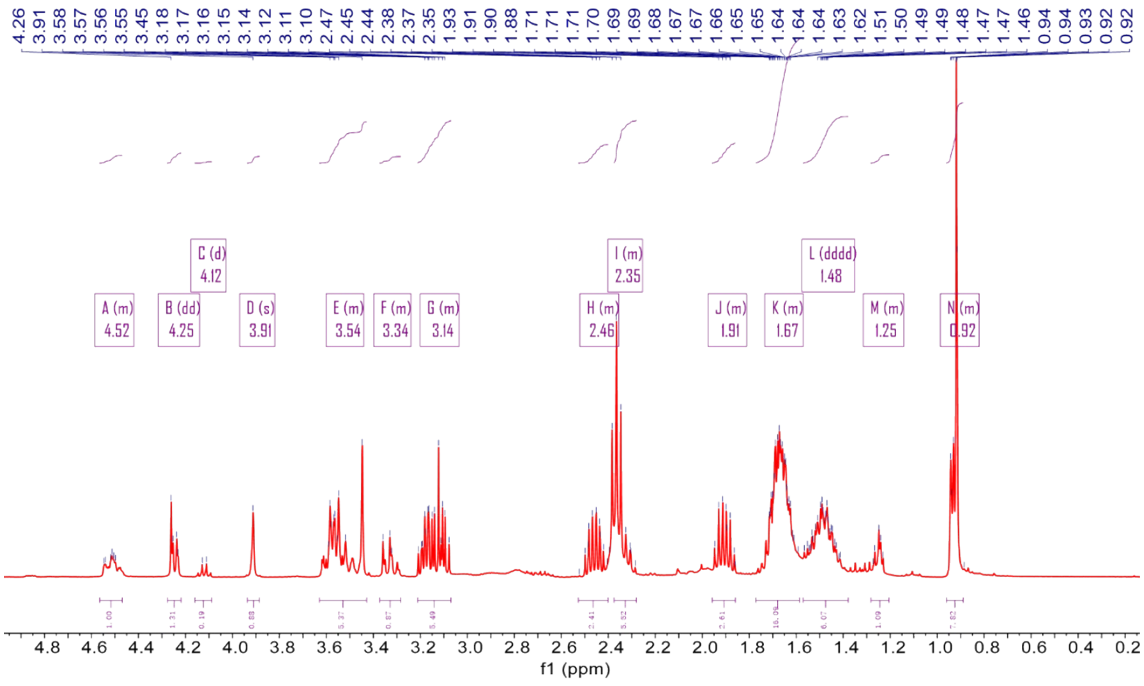

Figure S17. ^{1}H NMR spectrum of **TA-SPG$_{10\text{-}0.1\%}$ (recycling cycle 1)**. (400 MHz, $CDCl_3$, 298 K)

^{1}H NMR (400 MHz, Chloroform-*d*) δ 4.57 – 4.47 (m, 1H), 4.25 (dd, *J* = 9.1, 2.9 Hz, 1H), 4.12 (d, *J* = 7.2 Hz, 0H), 3.91 (s, 1H), 3.63 – 3.43 (m, 5H), 3.37 – 3.28 (m, 1H), 3.21 – 3.07 (m, 5H), 2.53 – 2.40 (m, 2H), 2.38 – 2.28 (m, 6H), 1.96 – 1.86 (m, 3H), 1.77 – 1.59 (m, 16H), 1.48 (dddd, *J* = 18.1, 13.3, 9.3, 7.0 Hz, 6H), 1.28 – 1.20 (m, 1H), 0.96 – 0.89 (m, 8H).

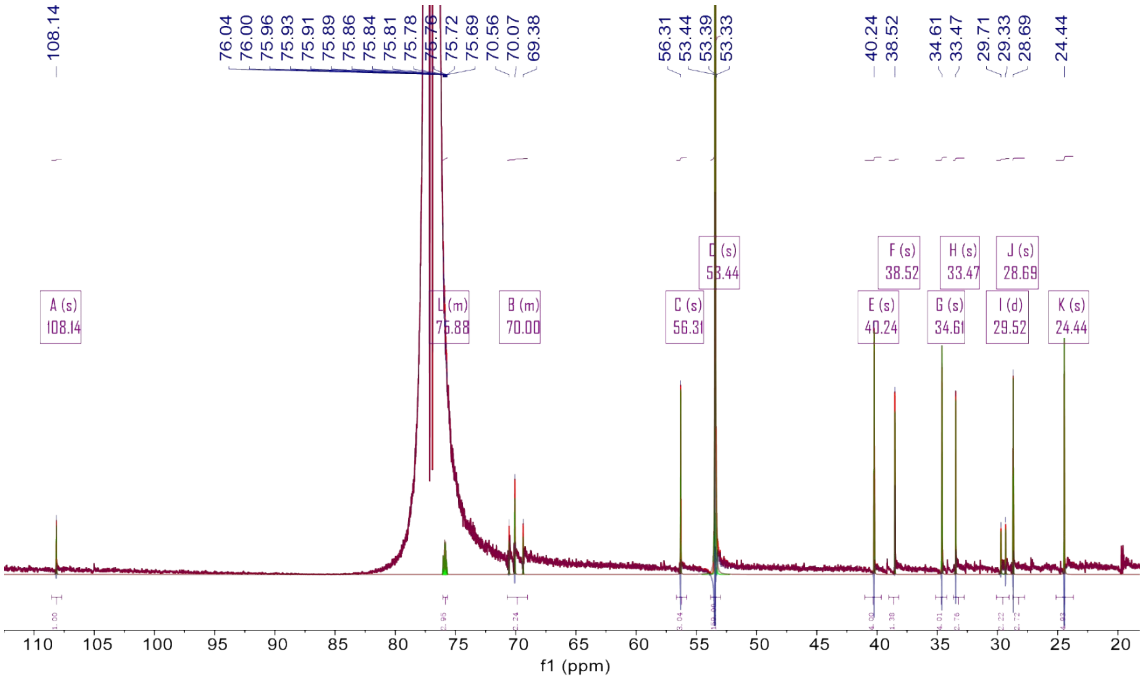

Figure S18. ^{13}C NMR spectrum of **TA-SPG$_{10\text{-}0.1\%}$ (recycling cycle 1)**. (600 MHz, $CDCl_3$, 298 K)

^{13}C NMR (151 MHz, Chloroform-*d*) δ 108.14, 76.04 – 75.65 (m), 70.70 – 69.02 (m), 56.31, 53.44, 40.24, 38.52, 34.61, 33.47, 29.52 (d, *J* = 57.4 Hz), 28.69, 24.44.

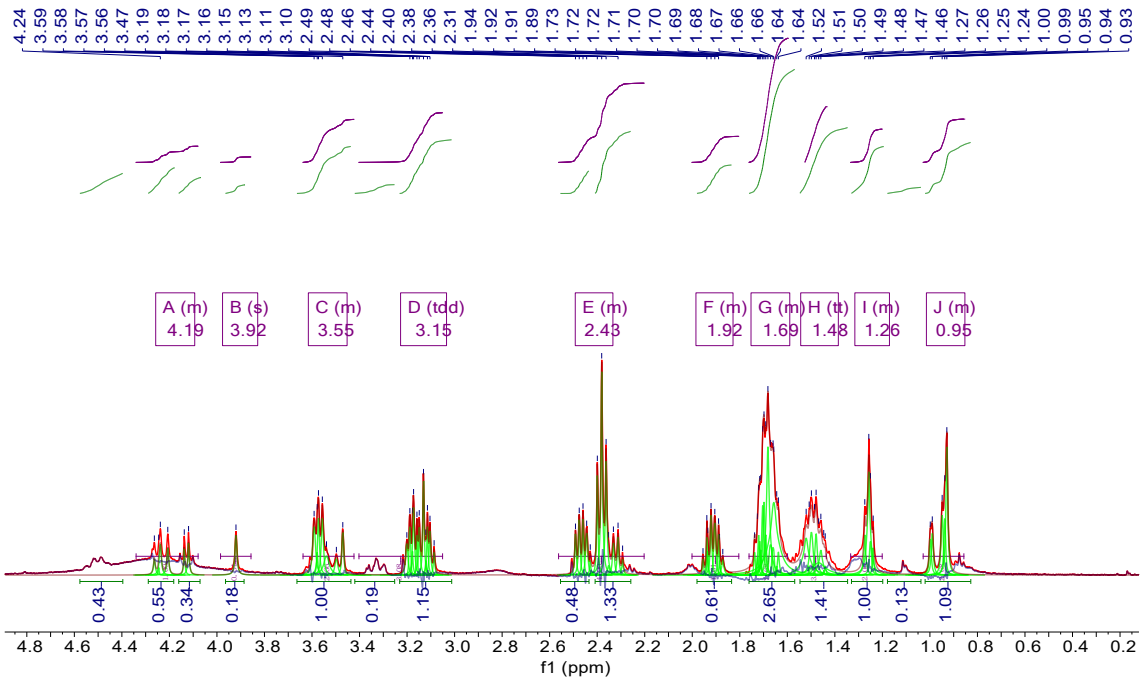

Figure S19. ^{1}H NMR spectrum of **TA-SPG$_{10\text{-}0.1\%}$ (recycling cycle 2)**. (400 MHz, $CDCl_3$, 298 K)

^{1}H NMR (400 MHz, Chloroform-d) δ 4.34 – 4.08 (m, 1H), 3.92 (s, 0H), 3.64 – 3.42 (m, 3H), 3.15 (tdd, J = 17.9, 10.4, 6.0 Hz, 3H), 2.56 – 2.20 (m, 5H), 2.00 – 1.80 (m, 2H), 1.76 – 1.60 (m, 8H), 1.48 (tt, J = 11.0, 6.2 Hz, 3H), 1.33 – 1.20 (m, 2H), 1.03 – 0.86 (m, 3H).

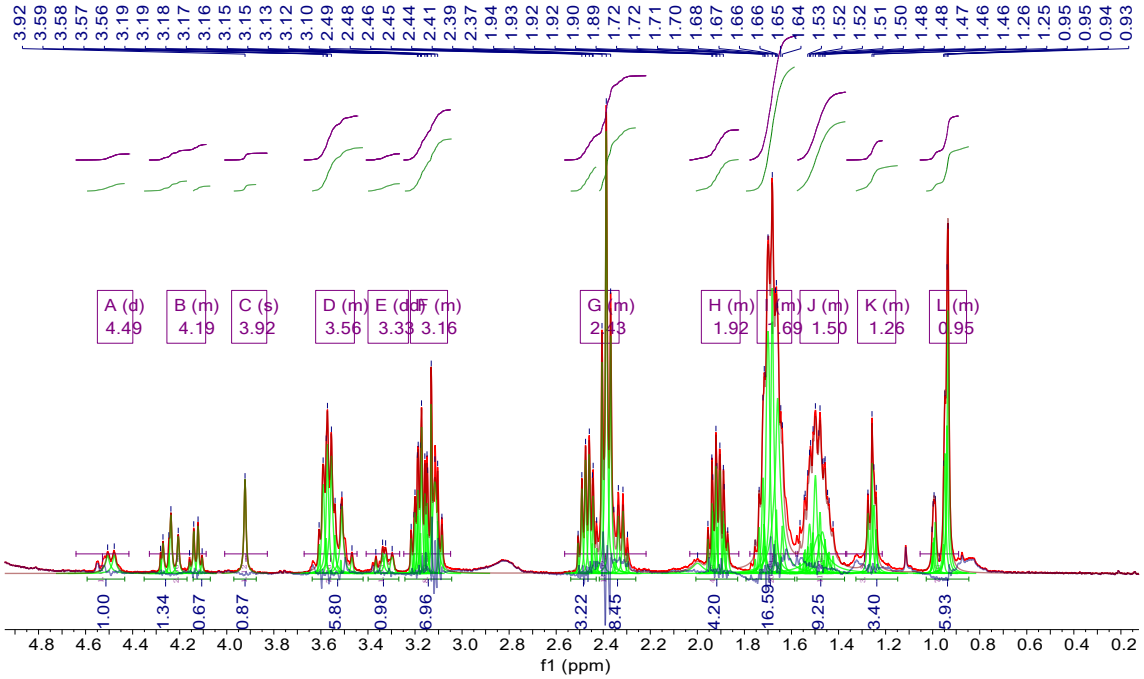

Figure S20. ^{1}H NMR spectrum of **TA-SPG$_{10\text{-}0.1\%}$ (recycling cycle 3)**. (400 MHz, $CDCl_3$, 298 K)

^{1}H NMR (400 MHz, Chloroform-*d*) δ 4.49 (d, *J* = 11.3 Hz, 1H), 4.33 – 4.09 (m, 3H), 3.92 (s, 1H), 3.67 – 3.45 (m, 7H), 3.33 (dd, *J* = 16.5, 11.3 Hz, 1H), 3.25 – 3.05 (m, 8H), 2.56 – 2.22 (m, 14H), 2.03 – 1.82 (m, 5H), 1.78 – 1.58 (m, 20H), 1.57 – 1.37 (m, 11H), 1.37 – 1.21 (m, 3H), 1.05 – 0.89 (m, 7H).

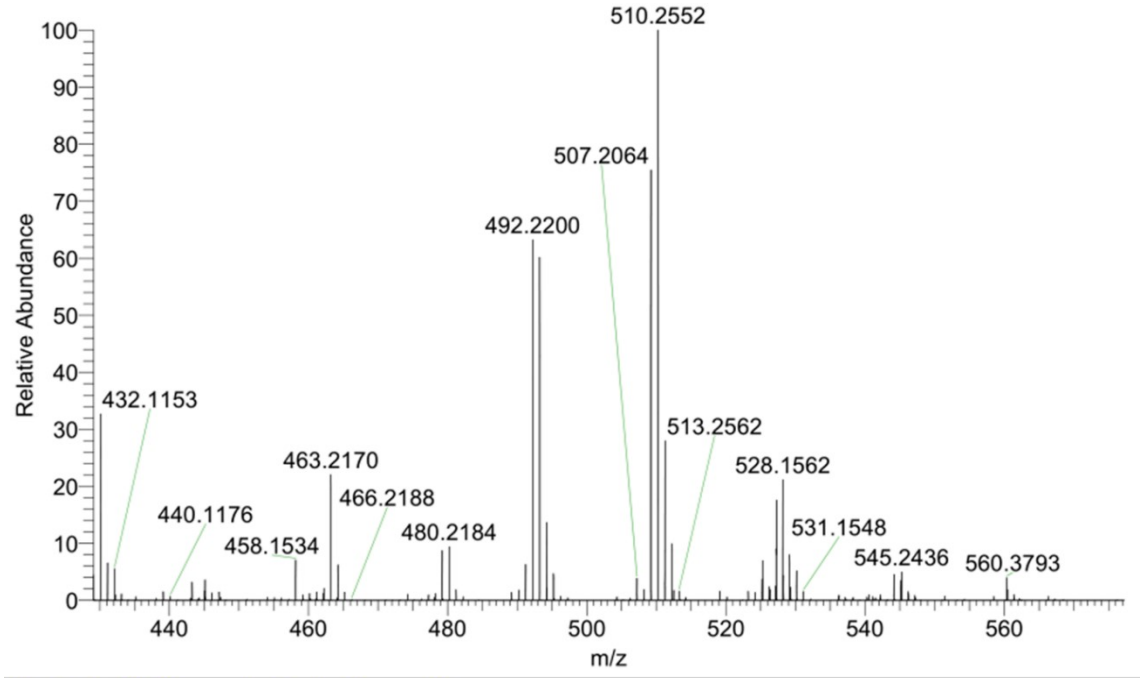

QD-YD-2#49-80 RT: 0.11-0.18 AV: 32
T: FTMS + p NSI Full ms [100.0000-1500.0000]
m/z= 491.67-492.43

m/z	Intensity	Relative	Theo. Mass	Delta (ppm)	Composition
492.2200	583843.1	100.00	492.2210	-0.98	$C_{23}H_{40}O_7S_2$

Figure S21. Mass spectrum of SPG mono in **TA-SPG$_{10\text{-}0.1\%}$ (recycling cycle 1)**.

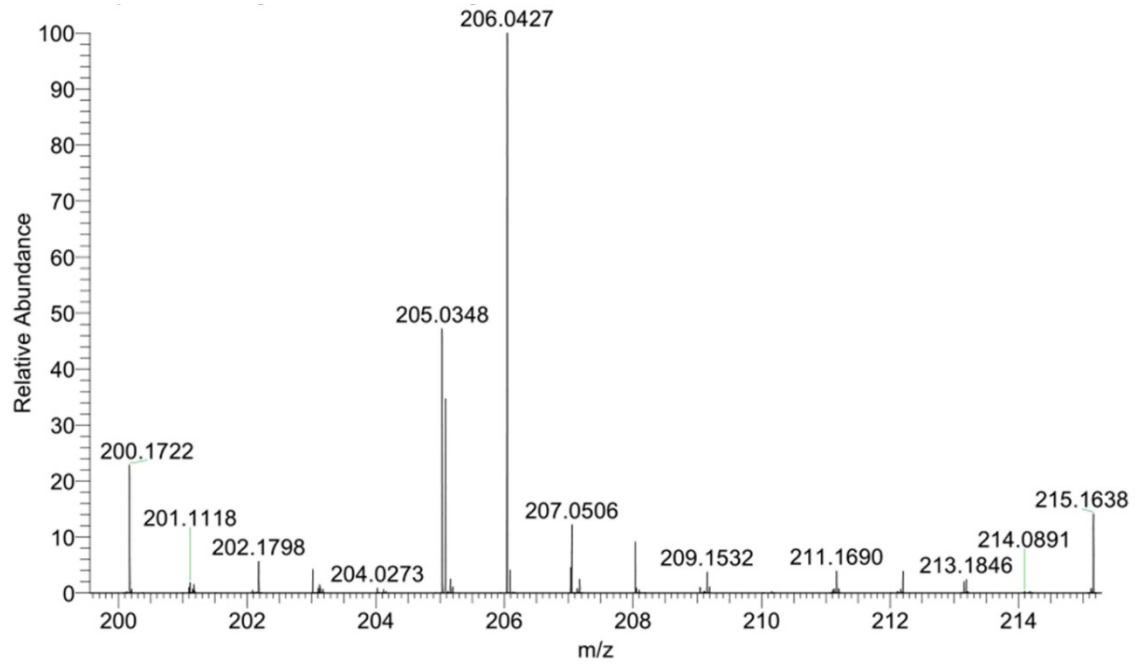

QD-YD-2#49-80 RT: 0.11-0.18 AV: 32
T: FTMS + p NSI Full ms [100.0000-1500.0000]
m/z= 205.97-206.15

m/z	Intensity	Relative	Theo. Mass	Delta (ppm)	Composition
206.0427	4553792.5	100.00	206.0430	-0.26	$C_8H_{14}O_2S_2$

Figure S22. Mass spectrum of TA mono in **TA-SPG$_{10\text{-}0.1\%}$ (recycling cycle 1)**.

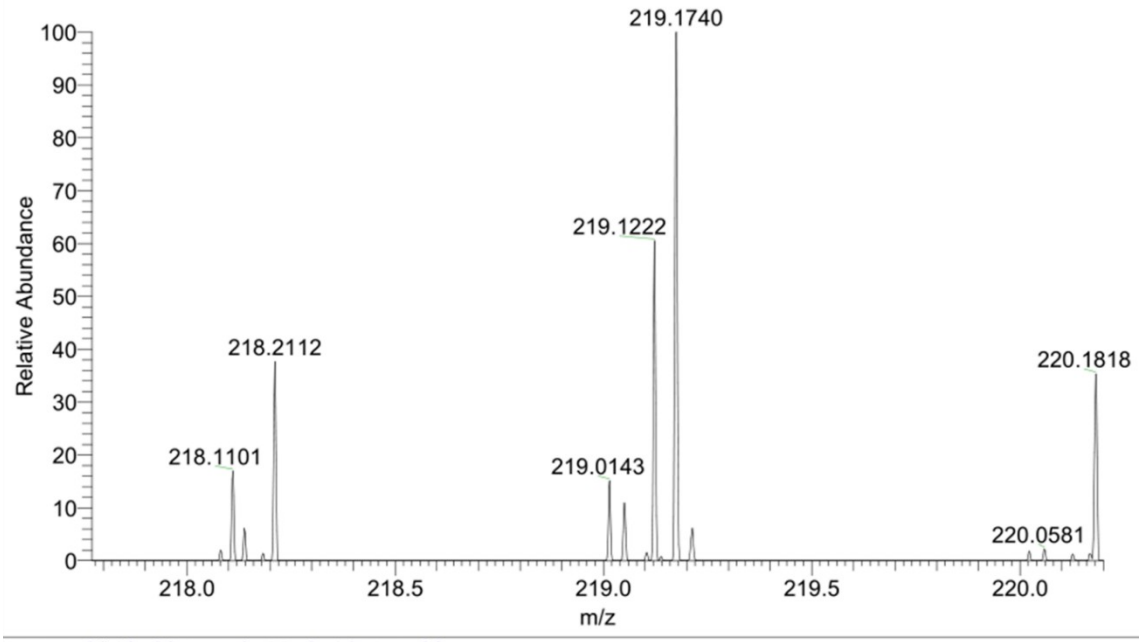

QD-YD-2#49-80 RT: 0.11-0.18 AV: 32
T: FTMS + p NSI Full ms [100.0000-1500.0000]
m/z= 219.00-219.02

m/z	Intensity	Relative	Theo. Mass	Delta (ppm)	Composition
219.0143	19671.8	100.00	219.0054	8.85	$C_9H_8O_4K$

Figure S23. Mass spectrum of caffeic acid in **TA-SPG$_{10\text{-}0.1\%}$ (recycling cycle 1)**.

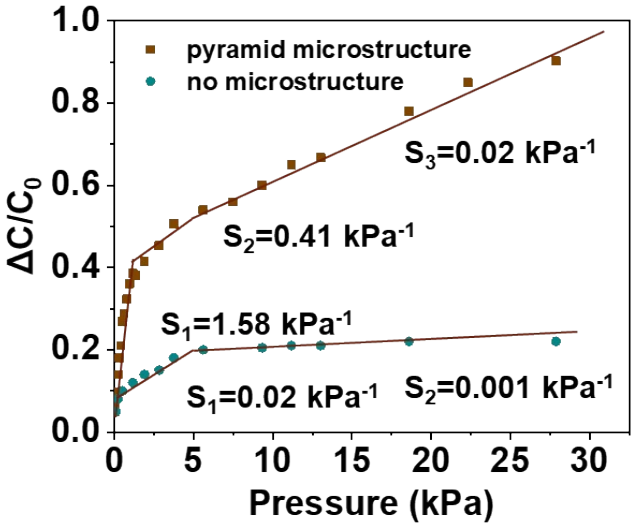

Figure S24. The sensor sensitivity comparisons of dielectric layer with and without pyramid microstructure.

Section III. Supporting Tables

Table S1. The summary of the tensile strength and elongation-at-break of all polymer.

Sample	Tensile strength (MPa)	Strain at break (%)	Toughness (MJ/m^3)
TA-SPG_5	1.50	15.98	0.1442
TA-SPG_{10}	0.05	39.83	0.0066
TA-$SPG_{10+0.1\%CA}$	0.03	151.75	0.0250
TA-$SPG_{10\text{-}5\%}$	0.33	243.87	0.4900
TA-$SPG_{10\text{-}0.1\%}$	1.26	195.52	2.1548
TA-$SPG_{10\text{-}0.5\%}$	0.83	166.53	1.0258

Table S2. Summarises tensile strength and elongation-at-break with different tensile rates of **TA-$SPG_{10\text{-}0.1\%}$**.

Sample	Tensile strength (MPa)	Strain at break (%)	Toughness (MJ/m^3)
10 mm/min	1.05	254.40	2.3584
20 mm/min	1.26	195.52	2.1548
50 mm/min	1.39	154.97	2.0988
100 mm/min	1.57	123.17	1.8436

Table S3. Self-healing mechanical properties of TA-SPG polymers.

Time (h)	Tensile strength (MPa)	Strain at break (%)	Toughness (MJ/m^3)
2	0.95	17.98	0.1101
4	0.91	47.28	0.3527
8	0.79	98.07	0.8499
10	1.06	144.22	1.3967
12	0.99	193.41	1.9394
virgin	1.21	196.18	2.1548

Table S4. Self-healing mechanical properties of **TA-SPG$_{10\text{-}0.1\%}$** polymers under different ambient humidity conditions.

Sample	Tensile strength (MPa)	Strain at break (%)	Toughness (MJ/m^3)
virgin	1.26	195.52	2.1548
0%	1.08	192.74	1.9070
50%	1.11	189.74	1.9394
70%	1.21	199.82	2.0281

Table S5. Multiple recycling cycles mechanical properties of **TA-SPG$_{10\text{-}0.1\%}$** polymers.

Sample	Tensile strength (MPa)	Strain at break (%)	Toughness (MJ/m^3)
virgin	1.26	195.52	2.1548
recycling cycle 1	1.13	187.89	2.0583
recycling cycle 2	1.12	196.04	1.9633
recycling cycle 3	1.12	185.39	1.7468

Table S6. Swelling ability in different solvents of **TA-SPG$_{10\text{-}0.1\%}$**.

Solvent	1 hour[a]	1 day[a]	1 week[a]	1 month[a]
Distilled water	0.0	1.6	5.4	9.1
Petroleum ether	0.1	3.4	1.0	8.8
Ethyl acetate	10.8	10.8	0.6	0.6
Dichloromethane	136.5	139.9	118.1	112.1
Acetone	31.7	◆	◆	●
Tetrahydrofuran	◆	◆	◆	◆
Ethanol	◆	◆	◆	●
Ethyl ether	2.2	16.3	20.0	1.9
Aqueous HCl[b]	10.6	5.7	8.4	6.4
Triethylamine	2.6	1.1	0.4	0.0

● *represents insoluble polymer chips*

◆ *represents insoluble polymeric powder*

a *Data for all samples was collected after being completely immersed in the chosen solvents for different time at ambient temperature*

b *The acid concentration was 0.05M*

Table S7. GPC data including Mn, Mw, and PDI of recycled **TA-SPG$_{10\text{-}0.1\%}$**.

	Mn	Mw	PDI
Recycled SPG mono	**904**	**1047**	**1.158**

Table S8. Signs of the main cross-peaks in 2DCOS.

Signs read in synchronous and asynchronous spectra, pesented as muplicity

1645	+	-	
1711	-		
1733			
	1733	1711	1645

Signs read in synchronous and asynchronous spectra, pesented as muplicity

3200	-	
3500		
	3500	3200